Supplementary Materials

Detailed Characterization of Thermal Runaway Particle Emissions from a Prismatic NMC622 Lithium-Ion Battery

Felix Elsner [1,*], Peter Gerhards [1], Gaël Berrier [2], Rémi Vincent [2], Sébastien Dubourg [3] and Stefan Pischinger [1]

[1] Chair of Thermodynamics of Mobile Energy Conversion Systems, RWTH Aachen University, D-52074 Aachen, Germany; gerhards@tme.rwth-aachen.de (P.G.); pischinger_s@tme.rwth-aachen.de (S.P.)
[2] University Grenoble Alpes, CEA, LITEN, DEHT, F-38000 Grenoble, France; gael.berrier@cea.fr (G.B.); remi.vincent@cea.fr (R.V.)
[3] CEA, DAM, Le Ripault, F-37260 Monts, France; sebastien.dubourg@cea.fr
* Correspondence: elsner@tme.rwth-aachen.de

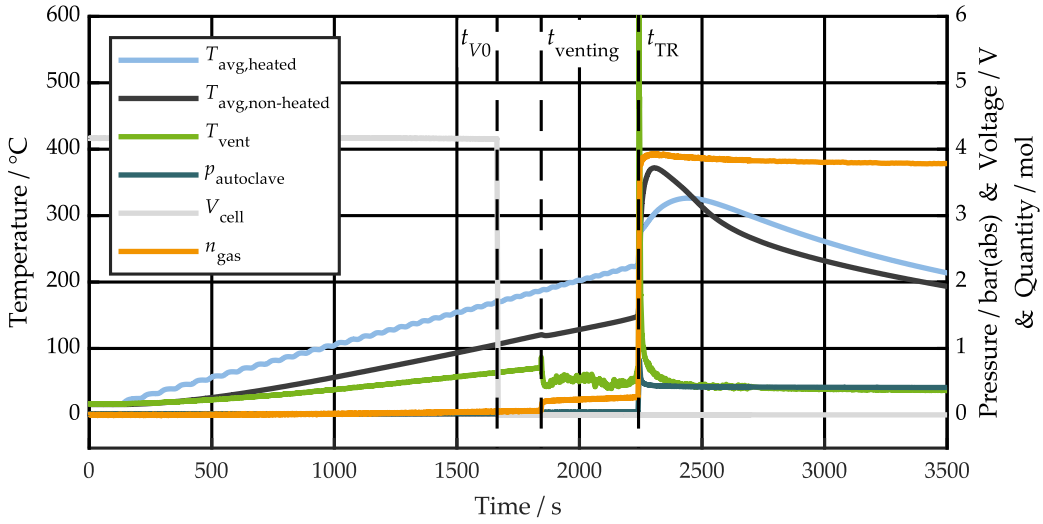


Figure S1. Time-dependent temperature T, pressure p, cell voltage V and gas quantity n profiles as well as characteristic timestamps for voltage drop t_{V0}, first venting $t_{venting}$ and thermal runaway t_{TR} for test #2.

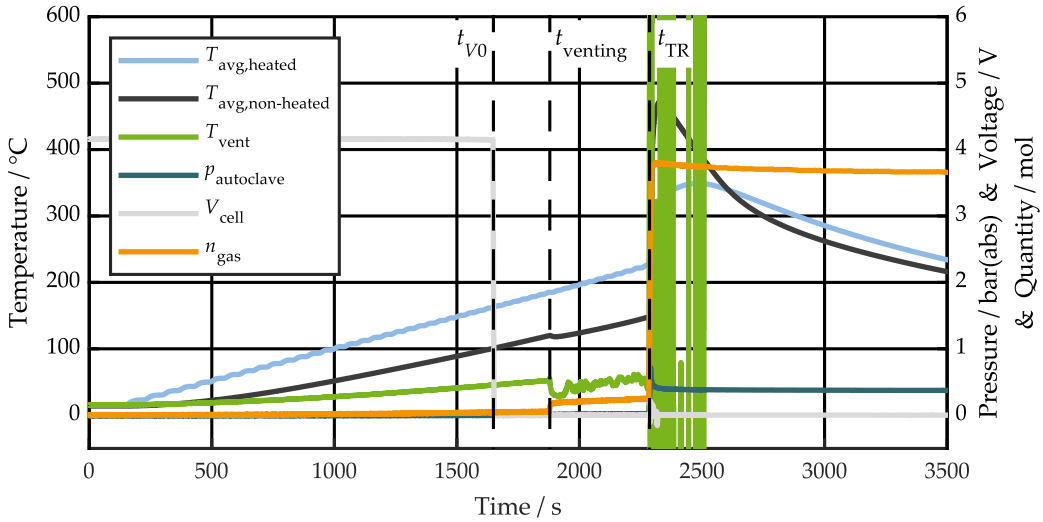


Figure S2. Time-dependent temperature T, pressure p, cell voltage V and gas quantity n profiles as well as characteristic timestamps for voltage drop t_{V0}, first venting $t_{venting}$ and thermal runaway t_{TR} for test #3.



Figure S3. Images of the cells after thermal runaway: (**a**) test #1, (**b**) test #2, (**c**) test #3.

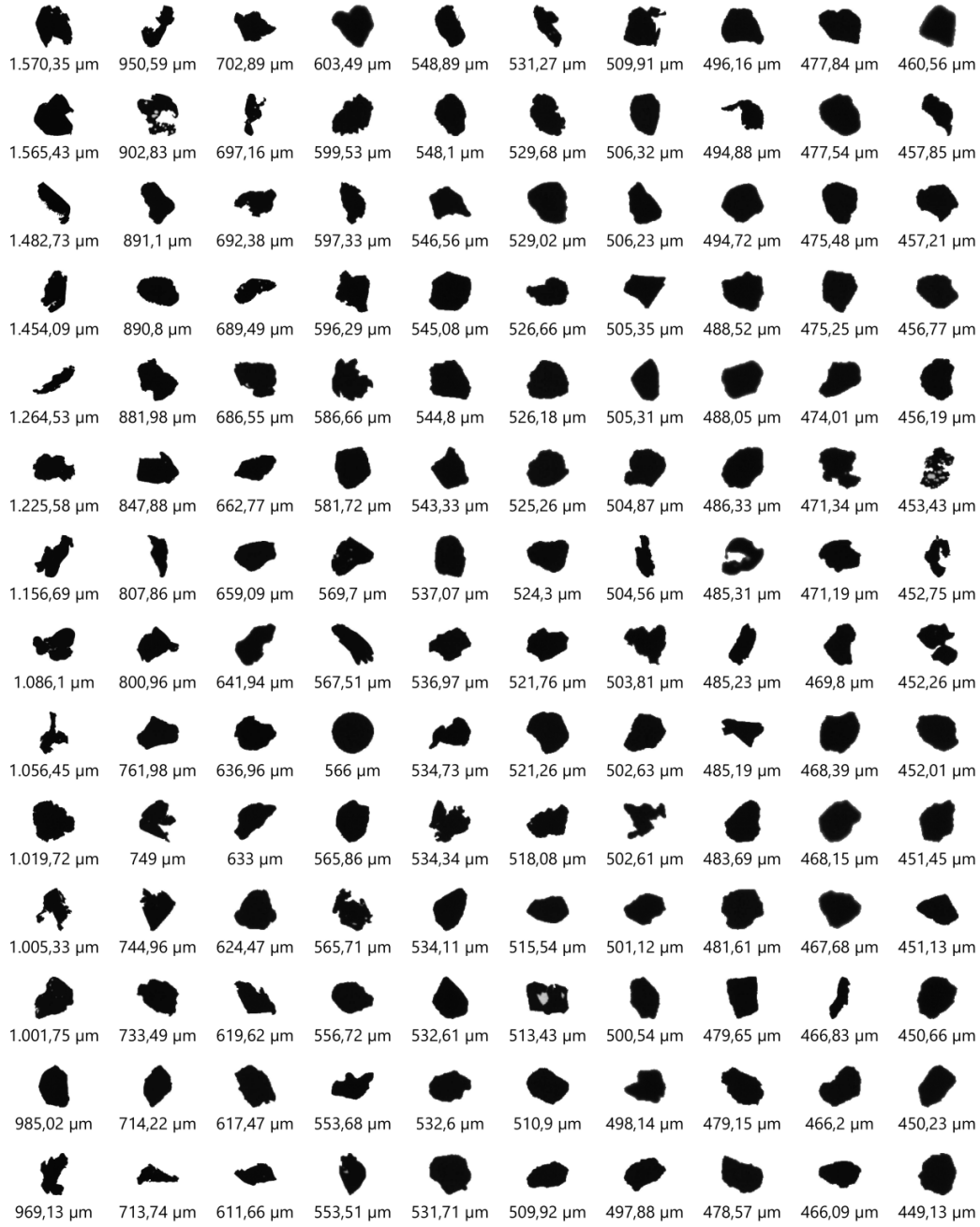


Figure S4. Particle images taken during the dynamic image analysis (DIA) of run #1.



Figure S5. Images of sorted copper-based (**a**) as well as aluminum-based, gray non-metallic, and "black" particles (**b**) > 2 mm from sample #1.

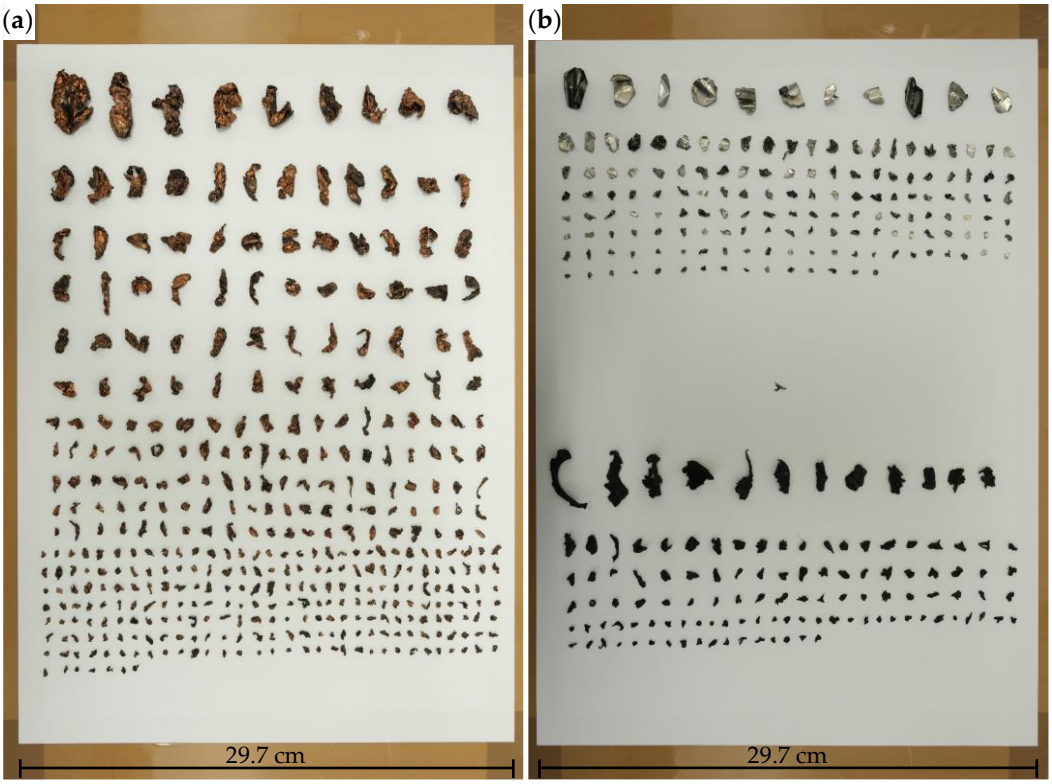


Figure S6. Images of sorted copper-based (**a**) as well as aluminum-based, gray non-metallic, and "black" particles (**b**) > 2 mm from sample #2.

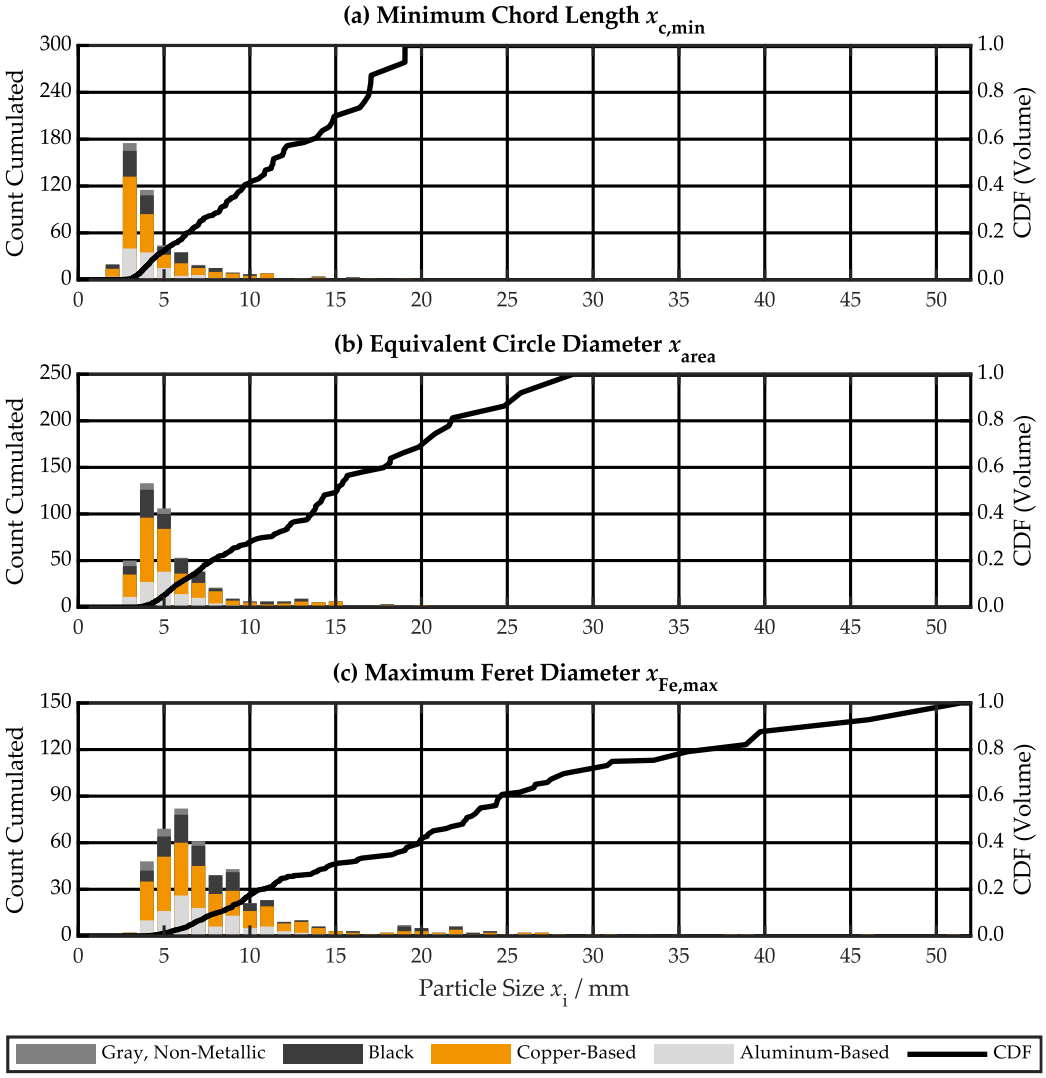


Figure S7. Large particle size characteristics split by material class as cumulated count and volume-specific cumulative distribution function (CDF) for sample #1: (**a**) minimum chord length $x_{c,min}$, (**b**) equivalent circle diameter x_{area}, (**c**) maximum Feret diameter $x_{Fe,max}$.

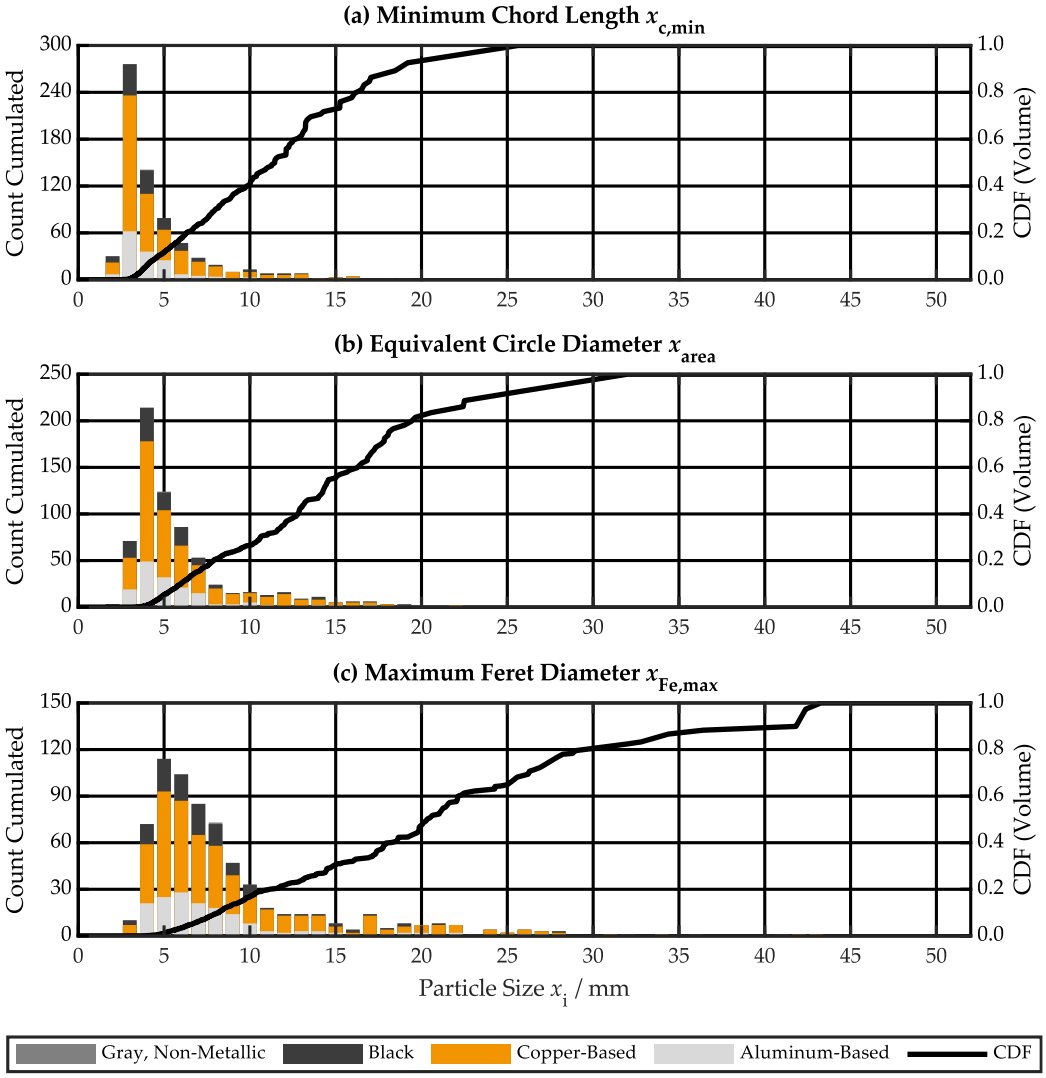


Figure S8. Large particle size characteristics split by material class as cumulated count and volume-specific cumulative distribution function (CDF) for sample #2: (**a**) minimum chord length $x_{c,min}$, (**b**) equivalent circle diameter x_{area}, (**c**) maximum Feret diameter $x_{Fe,max}$.

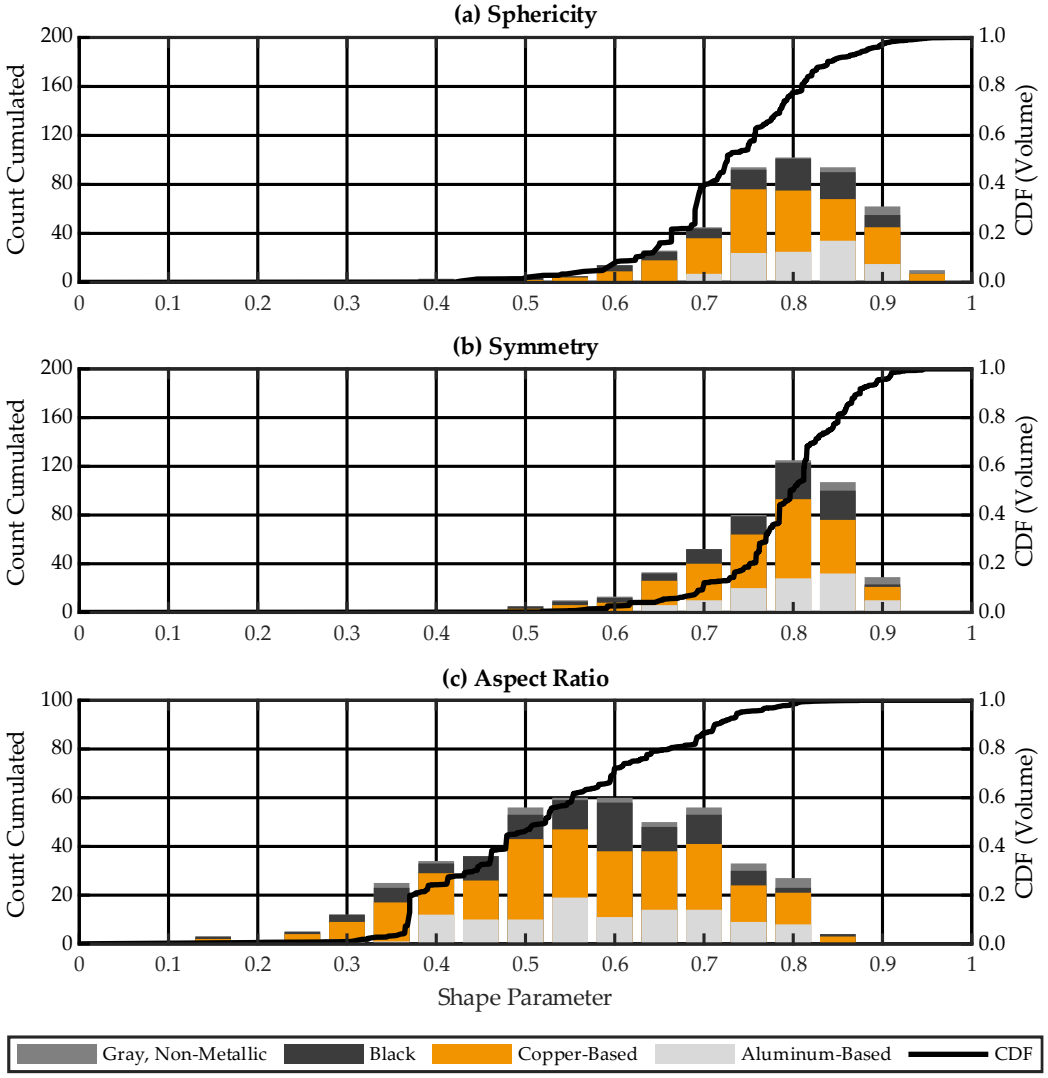


Figure S9. Large particle shape characteristics split by material class as cumulated count and volume-specific cumulative distribution function (CDF) for sample #1: (**a**) sphericity, (**b**) symmetry, (**c**) aspect ratio.

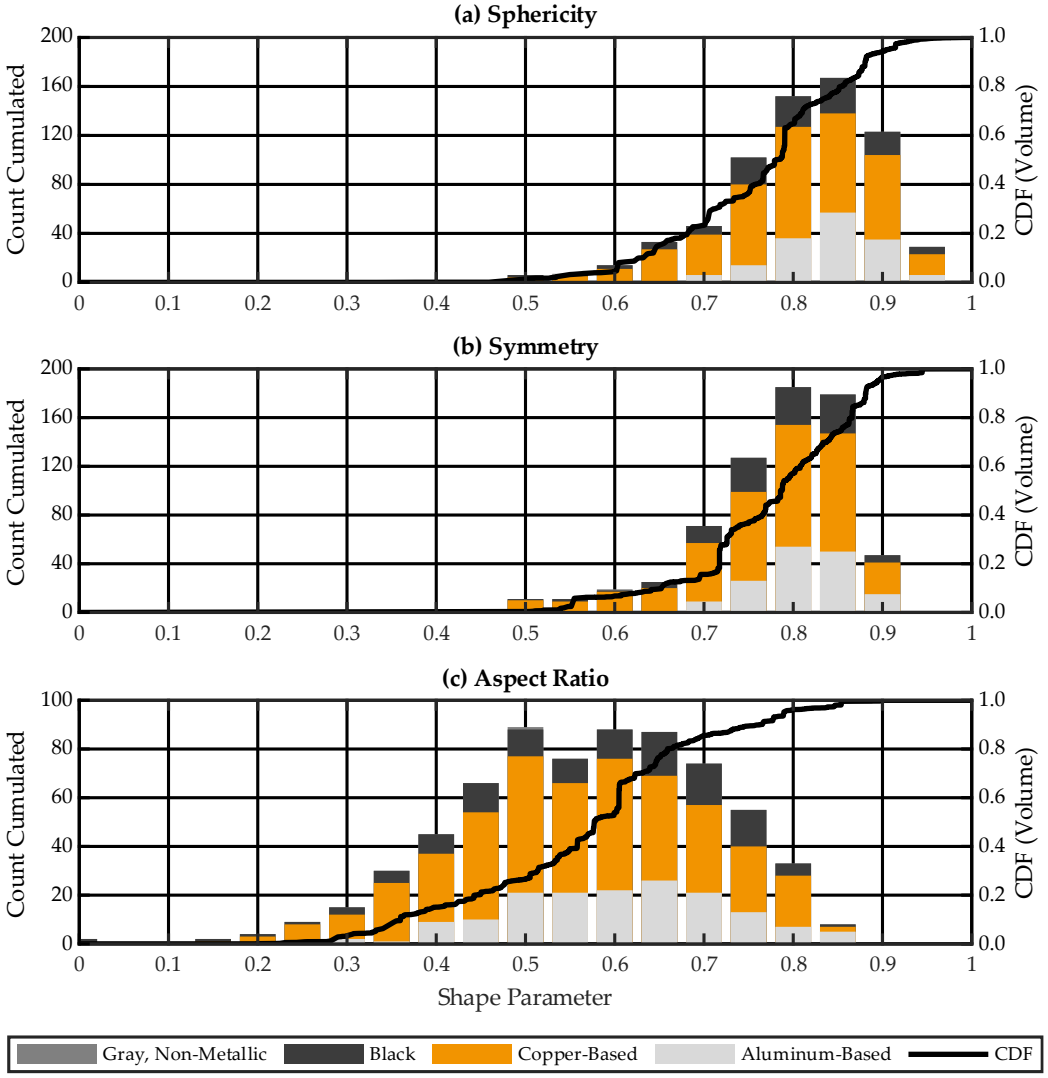


Figure S10. Large particle shape characteristics split by material class as cumulated count and volume-specific cumulative distribution function (CDF) for sample #2: (**a**) sphericity, (**b**) symmetry, (**c**) aspect ratio.

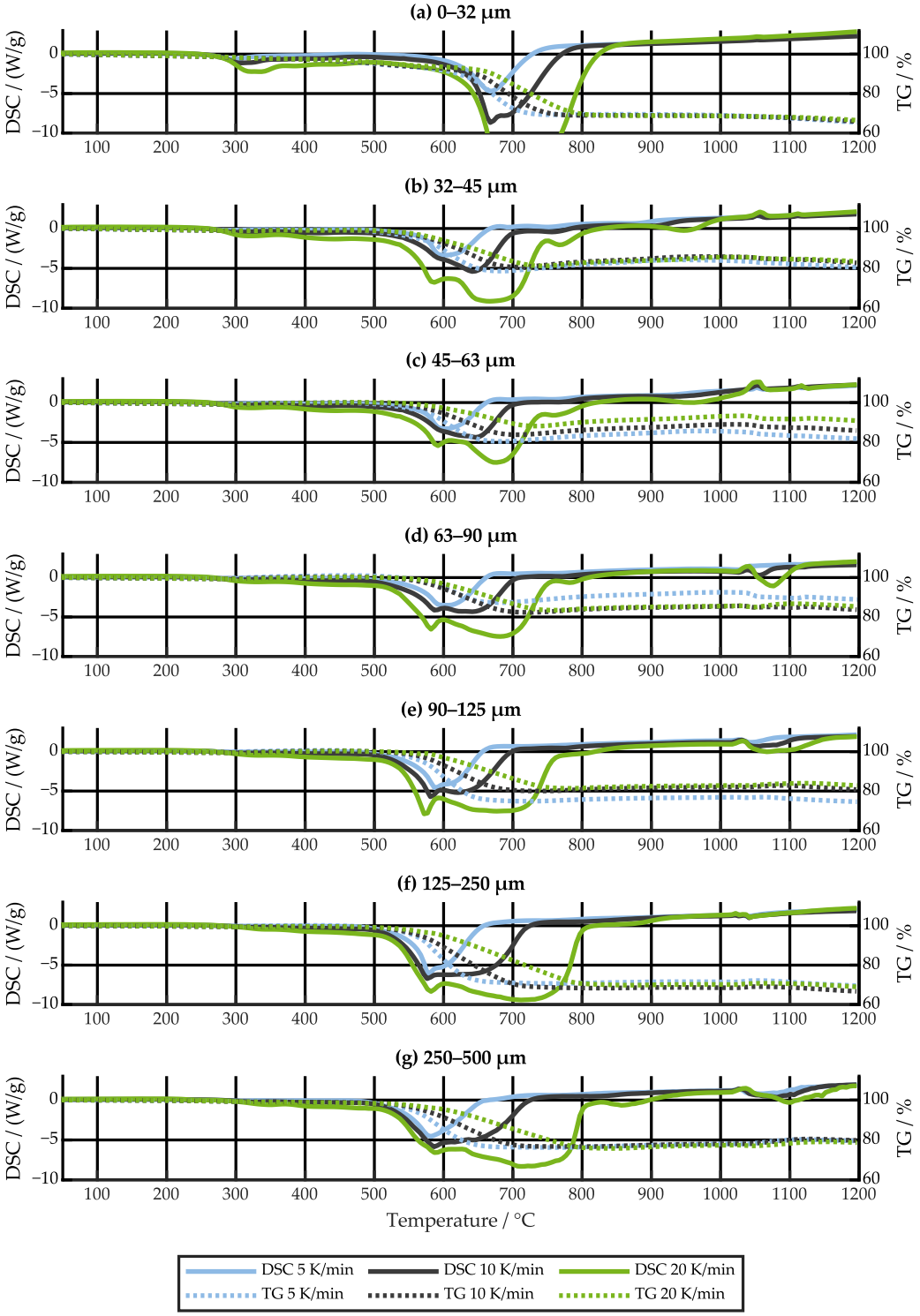


Figure S11. Differential scanning calorimetry (DSC) and thermogravimetric (TG) signals for different size fractions and heating rates.

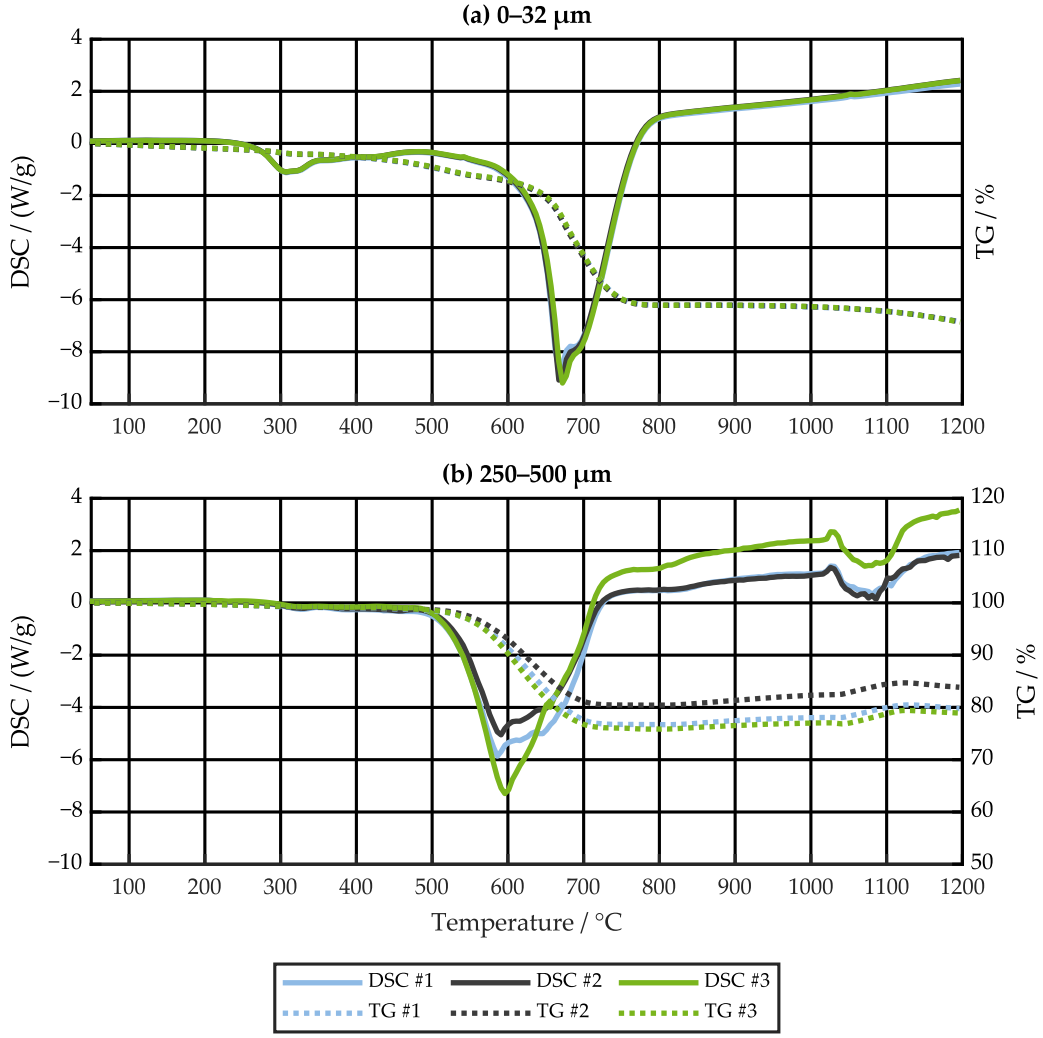


Figure S12. Differential scanning calorimetry (DSC) and thermogravimetric (TG) signals for three repetitive tests at a heating rate of 10 K/min: (**a**) size fraction 0–32 µm, (**b**) size fraction 250–500 µm.